IIETA International Information and Engineering Technology Association
Advancing the World of Information and Engineering

Traitement du Signal
Vol. 38, No. 2, April, 2021, pp. 261-268
Journal homepage: http://iieta.org/journals/ts

Multi-Sessions Outcome for EEG Feature Extraction and Classification Methods in a Motor Imagery Task

Oana-Diana Hrisca-Eva*, Anca Mihaela Lazar

Faculty of Medical Bioengineering, University of Medicine and Pharmacy "Grigore T. Popa" Iasi, Iasi 700115, Romania

Corresponding Author Email: oana.hrisca@umfiasi.ro

https://doi.org/10.18280/ts.380202

Received: 21 August 2020
Accepted: 20 March 2021

Keywords:
electroencephalogram, motor imagery, features extraction, autoregressive process, amplitude modulation, phase synchronization, classification algorithms

ABSTRACT

The purpose of this research is to evaluate the performances of some features extraction methods and classification algorithms for the electroencephalographic (EEG) signals recorded in a motor task imagery paradigm. The sessions were performed by the same subject in eight consecutive years. Modeling the EEG signal as an autoregressive process (by means of Itakura distance and symmetric Itakura distance), amplitude modulation (using the amplitude modulation energy index) and phase synchronization (measuring phase locking value, phase lag index and weighted phase lag index) are the methods used for getting the appropriate information. The extracted features are classified using linear discriminant analysis, quadratic discriminant analysis, Mahalanobis distance, support vector machine and k nearest neighbor classifiers. The highest classifications rates are achieved when Itakura distance with Mahalanobis distance based classifier are applied. The outcomes of this research may improve the design of assistive devices for restoration of movement and communication strength for physically disabled patients in order to rehabilitate their lost motor abilities and to improve the quality of their daily life.

1. INTRODUCTION

Brain computer interface (BCI) is the technology that acquires, analyses and translates brain signals into commands in order to control an external device [1].

Electroencephalography (EEG) records the brain signals noninvasively with electrodes placed on the scalp [2].

The aim of BCI based EEG was to offer a better communication way for persons with motor disabilities through evaluation and classification of features contained in the EEG signals.

Sensorimotor rhythms are those EEG rhythms related to motor actions such as preparing, movement or even imagining a limb movement. These actions determine changes in the brain activity. The sensorimotor rhythms are located over the motor cortex in the frequency bands 8–13 Hz (rhythm Mu) and 13–30 Hz (rhythm Beta).

Motor imagery (MI) is the translation of the subject's motor intention through motor imagery states [3].

Various forms of electrical brain activities [4] have been used for EEG based BCI systems. Mu rhythm [5-7], P300 [8, 9], steady state visual evoked potential [10-12] are some of them.

The most successful feature extraction methods widely used are: common spatial pattern [13], Fourier transform [14], independent component analysis [15], phase synchronization [16], wavelet transform [17] and autoregressive (AR) spectral estimation [18].

Many studies were performed in order to establish which the most convenient method is for extraction the important features from certain EEG signals recorded in sessions from the same day. The purpose of this research is to look for the changes that appeared during a period of eight years from a single female subject which has performed a motor imagery paradigm.

The remainder of this paper is organized as follows: Section 2 describes the EEG recordings, Section 3 details the applied features extraction methods, Section 4 presents the results and Section 5 the conclusions.

2. EEG RECORDINGS

The experiments were performed in the Signal Processing Laboratory from the Faculty of Medical Bioengineering. The acquisition system was composed from a gMobilab+ module, a g.GAMMAcap, a g.GAMMAbox [19] and the BCI 2000 platform [20].

The electrodes were placed in C3, C4, P3, P4, CP3, CP4, Cz and Pz positions according to International 10-20 System and the reference electrode on the right ear. The sampling frequency was 256 Hz.

Sitting comfortably in front of a PC monitor, the subject tried to imagine the hand movement indicated by the displayed arrow. If it was displayed a left/right oriented arrow, the subject had to imagine the left/right hand movement. The arrows were randomly displayed 30 times. When the screen was white, the subject had to relax. Before each session, the subject was trained by performing a trail with left and right hand movements instead of imaging the movement.

In order to assess the efficiency of some of the feature extraction and of the classification methods, EEG signals recorded from the same person during the period of eight years (2012 – 2019) were handled. The EEG recordings were acquired in different hours, days, months and years in illumination conditions chosen by the subject (Table 1).

Table 1. The EEG recordings grouped by month and year

Session	Month	Year
1	November	2012
2	November	2013
3	December	
4	November	2014
5	March	2015
6	March	
7	April	2016
8	May	
9	May	2017
10	April	2018
11	April	2019

3. FEATURE EXTRACTION AND CLASSIFICATION METHODS

Three methods are taken into account: modeling the EEG signal as an autoregressive process, amplitude modulation and phase synchronization. The handled measures are: the Itakura distance for the autoregressive process, the amplitude modulation energy index for the amplitude modulation and phase locking value (PLV), phase lag index (PLI) and weighted phase lag index (wPLI) to estimate the synchronization between two EEG signals.

In what follows, the main aspects of the proposed methods will be highlighted. The detail descriptions for an interested reader are found in Ref. [21-26].

Three EEG datasets were created: one for right hand movement imagination, $y_{RIGHT}(n)$, one for left hand movement imagination, $y_{LEFT}(n)$, and one for relaxation, $y_{REST}(n)$.

For further processing, the frequency band 8 – 12 Hz (Alpha rhythm) was considered.

3.1 Autoregressive process

As it is already known, an EEG signal, denoted by $y(n)$, can be considered as the output of an AR process described by the expression:

$$y(n) = -\sum_{k=1}^{p} a_k y(n-k) + n(n) \tag{1}$$

where, a_k are the parameters of the model, p is the model order and $n(n)$ the unpredictable part of the EEG signal $y(n)$.

The best AR model may be obtained by minimizing the mean square error (MSE). It is shown that [21] the minimum MSE is:

$$MSE_y = a^T R_y(p) a \tag{2}$$

where, $a = \left[1\ a_1\ a_2 \dots a_p\right]^T$, $R_y(p)$ is the autocorrelation matrix of $y(n)$, and T the transpose of a matrix.

Passing the $y_{REST}(n)$ signal through AR(p) model caracterized by the a^{REST} parameters, the minimum MSE is:

$$MSE_{y_{REST},a^{REST}} = (a^{REST})^T R_{y_{REST}}(p) a^{REST} \tag{3}$$

and passing the same signal through any other AR(p) model, caracterized by a^{RIGHT} or by a^{LEFT} gives the MSEs as:

$$MSE_{y_{REST},a^{RIGHT}} = (a^{RIGHT})^T R_{y_{REST}}(p) a^{RIGHT} \tag{4}$$

$$MSE_{y_{REST},a^{LEFT}} = (a^{LEFT})^T R_{y_{REST}}(p) a^{LEFT} \tag{5}$$

Any of the MSEs from (4) or (5) is higher or equal then $MSE_{y_{REST},a^{REST}}$ from (3). The equality occurs when the AR models for relaxation period is the same for imagination of the right/left hand movement. The larger the deviation from the AR model from the relaxation period is, the more significant changes in the EEG signal from the EEG during relaxation are.

The Itakura distance (ID) measures the similarity between right/left hand movement imagination and the relaxation state. So, for imagination of the right hand, ID is defined by:

$$ID_{REST-RIGHT} = \log\left(\frac{MSE_{y_{REST},a^{RIGHT}}}{MSE_{y_{REST},a^{REST}}}\right) \tag{6}$$

and for the left by:

$$ID_{REST-LEFT} = \log\left(\frac{MSE_{y_{REST},a^{LEFT}}}{MSE_{y_{REST},a^{REST}}}\right) \tag{7}$$

The two classes formed for further processing are $ID_{REST-RIGHT}$ and $ID_{REST-LEFT}$.

The symmetric Itakura distance, ID_{RIGHT}, for imagination of right hand movement (using (6) and a relation similar to it) is [22]:

$$ID_{RIGHT} = \frac{1}{2}(ID_{REST-RIGHT} + ID_{RIGHT-REST}) \tag{8}$$

and for movement of left hand movement, ID_{LEFT}, using (7) and a relation similar to it, is:

$$ID_{LEFT} = \frac{1}{2}(ID_{REST-LEFT} + ID_{LEFT-REST}) \tag{9}$$

Both for ID and symmetric ID the model order p=6 and model order p=10 was evaluated.

The data contained on channels C3 and C4 and frequency band 8 – 12 Hz were chosen.

3.2 Amplitude modulation

The amplitude modulation analysis allows for understanding which modulation frequencies ride a cerebral rhythm over short periods of time. From the five rhythms (Delta, Theta, Alpha, Beta and Gamma), only the EEG signal from *Alpha* rhythm is handled here as the best results were found for this band.

The temporal amplitude envelope is computed by means of Hilbert transform [23].

The Hilbert transform $\mathcal{H}\{.\}$ of $y_{RIGHT}(n)$ EEG signal is described by:

$$\mathcal{H}\{y_{RIGHT}(n)\} = \frac{1}{\pi} PV \int_{-\infty}^{+\infty} \frac{y_{RIGHT}(n)}{t-\pi} dt \tag{10}$$

where, PV is the Cauchy principal value.

The analytic signal $y_{RIGHT}(n)_a$ is defined as:

$$y_{RIGHT}(n)_a = y_{RIGHT}(n) + j\mathcal{H}\{y_{RIGHT}(n)\} \tag{11}$$

The amplitude modulation (or the temporal amplitude envelope) for $y_{RIGHT}(n)_a$, represented by $R_{AM}(n)$, is defined as:

$$R_{AM}(n) = \sqrt{y_{RIGHT}(n)^2 + \mathcal{H}\{y_{RIGHT}(n)\}^2} \quad (12)$$

$R_{AM}(n)$ is multiplied by a 5 s Hamming window with 0.5 s delay and is obtained the temporal envelope for frame m, expressed by $R_{AM}(m,n)$.

Then the modulus of the Fourier transform of the amplitude modulation for frame *m* is computed:

$$R_{AM}(m,f) = |\mathcal{F}\{R_{AM}(m,n)\}| \quad (13)$$

where, *f* is the modulation frequency and $\mathcal{F}\{R_{AM}(m,n)$ is the discrete Fourier transform of $R_{AM}(m,n)$.

The energy of the j modulation band, denoted by $RE_j(m,f)$, is computed as:

$$RE_j(m,f) = R_{AM_j}(m,f)^2 \quad (14)$$

and the average of energies over all the frames, expressed by $\overline{RE_j(m,f)}$.

The amplitude modulation energy index of the j modulation band [27], $REI_j(f)$, is defined by the following expression:

$$REI_j(f) = \frac{\overline{RE_j(m,f)}}{\sum_{j=1}^{k} \overline{RE_j(m,f)}} \quad (15)$$

where, *k* is the number of the modulation bands for the rhythm taken into account. For *Alpha* rhythm, k=3, because there are possible delta, theta, and alpha modulation bands.

3.3 Phase synchronization

The phase locking value represents the stability of the phase difference between instantaneous phases $\varphi_x(t)$ and $\varphi_y(t)$, and it is expressed as:

$$PLV = \left|\langle e^{j\Delta\varphi(t)}\rangle\right| \\ \Delta\varphi(t) = \varphi_y(t) - \varphi_x(t) \quad (16)$$

The phase lag index [25] is stated as:

$$PLI = |\langle sign[\Delta\varphi(t_k)]\rangle| \quad (17)$$

$sign$ is the signum function and $\langle . \rangle$ denotes the average over the time.

The weighted phase lag index is determined by [26]:

$$wPLI = |\langle I(X)\rangle|/\langle |I(X)|\rangle = \frac{|\langle |I(X)| sign\, I(X)\rangle|}{\langle |I(X)|\rangle} \quad (18)$$

where, $I(X)$ is the imaginary part of the cross spectrum between signals $x(t)$ and $y(t)$.

In order to compute the phase synchronization parameters, four combinations Cz-C3, Cz-C4, Pz-C3 and Pz-C4 were taken into account.

The above described methods were conducted also for left hand movement imagination.

3.4 Classifiers

Discrimination between right hand movement imagination and left hand movement imagination was assessed using linear discriminant analysis (LDA), quadratic discriminant analysis (QDA), Mahalanobis distance (MD), k nearest neighbor (kNN) with k=5 and support vector machine (SVM) classifiers [28-33]. A 5x5 fold cross validation procedure estimated the classification rate, specificity and sensitivity for the sessions performed by the subject.

The terms commonly used for the description of sensitivity, specificity and classification rate are: true positive (TP), true negative (TN), false negative (FN) and false positive (FP).

The classification rate, specificity and sensitivity [34] are defined by:

$$Sensitivity = \frac{TP}{TP + FN} \quad (19)$$

$$Specificity = \frac{TN}{TN + FP} \quad (20)$$

$$Classification\ rate = \frac{TN + TP}{TN + TP + FN + FP} \quad (21)$$

4. RESULTS

In Table 2 and Table 3 are displayed the classification rates, sensitivity, specificity (%) for Itakura Distance (model order 6 and model order 10) obtained with all the classifiers. The highest classification rates of 93.33%, for both orders, were attained with Mahalanobis distance classifier.

In Table 4 and Table 5 are shown the performance of classifiers for symmetric Itakura Distance (model order 6 and model order 10, respectively) with the same classifiers as in the previous cases. In these situations, the highest classification rates of 90% and 91.67% for model order 6, and model order 10 respectively, were achieved with quadratic discriminant analysis.

The classification rates (%), the sensitivities (%) and the specificities (%) for *Alpha_Alpha* and *Theta_Alpha* (the first word meaning the modulation band and the second the rhythm) with all the classifiers are displayed in Table 6.

The highest classification rates for *Alpha_Alpha* and *Theta_Alpha* were obtained with k nearest neighbor classifier. The classification rates attained for *Theta_Alpha* were smaller than the classification rates obtained for *Alpha_Alpha*. The most consistent results were obtained for session 9. In Table 7 are represented the classification rates, sensitivity and specificity for phase locking value. The highest performances were obtained with k nearest neighbor classifier (85.06%, 84.82% and 83.06% for classification rate, sensitivity and specificity, respectively, in session 8).

The classification rates, sensitivity and specificity realized for PLI are depicted in Table 8 and it is easy to see that the best performances are for k nearest neighbor classifier, for session 8 (classification rate of 85.16%, sensitivity of 87.16% and specificity of 78.85%).

In Table 9 are detailed the results for weighted phase lag index. The results are inferior to those for phase locking value and phase lag index.

So, for phase synchronization, the best performances are similar for phase locking value and phase lag index using k nearest neighbor classifier for the same session, with the remark that the specificity was lower for phase lag index.

Because no significant performances were found due to subject's practice, the calculus of the average values for

classification rates, sensitivities and specificities of all the sessions makes sense. In Figure 1, Figure 2 and Figure 3 are displayed the mean of the classification rates, of the sensitivities and of the specificities, for all proposed feature extraction methods and classifiers.

The best result for the mean of classification rates, 80.05% was achieved using amplitude modulation energy index for amplitude modulation method (alpha rhythm in alpha modulation band) and k nearest neighbor classifier. A close result was found for autoregressive process by means of Itakura distance of order 6 and Mahalanobis distance classifier, when 79.39% was attained. The k nearest neighbor classifier and amplitude modulation with amplitude modulation energy index (in case of theta modulation band) and phase synchronization method by means of phase locking value and phase lag index as feature vectors, were also achieved very good results (78.26%, 79.3% and 78.12%, respectively).

Table 2. Classification rates, sensitivities, specificities (%) for Itakura distance (model order 6)

		Session										
		1	**2**	**3**	**4**	**5**	**6**	**7**	**8**	**9**	**10**	**11**
Classification rates (%)	**LDA**	56.67	81.67	63.33	71.67	56.67	80	56.67	65	85	68.33	80
	QDA	73.33	91.67	61.67	88.33	70	88.33	83.33	71.67	88.33	70	78.33
	MD	71.67	**93.33**	71.67	90	68.33	86.67	86.67	71.67	88.33	68.33	76.67
	SVM	58.33	90	70	78.33	66.67	90	76.67	78.33	88.33	70	76.67
	kNN	64.17	89.72	54.17	88.06	58.61	86.67	81.67	73.89	84.17	67.5	76.67
Sensitivity (%)	**LDA**	39.72	92.06	73.61	83.33	62.33	67.44	84.83	57.83	81.56	46	91.11
	QDA	80	**97**	84.83	95.72	69.61	92.44	83.33	78.44	91.78	49.61	91.11
	MD	63.44	92.72	70.33	95.72	56.72	96.72	83.33	85.17	91.78	35.56	89.61
	SVM	71.19	90.01	65.69	83.91	55.89	85.1	81.66	73.49	80.38	71.94	71.04
	kNN	75.03	93.24	56.77	91.02	56.57	88.46	85.9	73.74	88.17	57.78	78.31
Specificity (%)	**LDA**	79.61	75.61	47	57.56	38.67	87.33	46.17	57.06	87.17	81.61	82
	QDA	68.5	90.5	50.67	88.78	65.89	81.22	86.94	63	87.17	81.44	81.33
	MD	75.78	**97.39**	79.17	93.06	76.72	71	89.11	52.94	87.17	92.61	81.33
	SVM	59.38	85.98	64.01	87.54	54.7	84.38	82.57	77.04	88.91	68.71	71.61
	kNN	59.96	89.1	51.22	88.62	61.03	84.74	84.58	76.23	83.47	78.59	82.39

Table 3. Classification rates, sensitivities, specificities (%) for Itakura distance (model order 10)

		Session										
		1	**2**	**3**	**4**	**5**	**6**	**7**	**8**	**9**	**10**	**11**
Classification rates (%)	**LDA**	48.33	81.67	60	75	61.67	91.67	61.67	81.67	91.67	76.67	88.33
	QDA	45	85	66.67	76.67	70	90	66.67	83.33	91.67	76.67	90
	MD	51.67	81.67	63.33	83.33	68.33	90	71.67	81.67	**93.33**	76.67	83.33
	SVM	31.67	83.33	75	81.67	68.33	88.33	66.67	85	91.67	81.67	88.33
	kNN	52.5	81.67	67.78	75.83	70.28	92.5	69.17	83.06	92.78	77.78	83.06
Sensitivity (%)	**LDA**	37.78	94.78	64.94	77.89	63.67	81.67	85.17	61.39	93.28	71.06	**100**
	QDA	19.44	95.06	73.33	77.89	74.72	81.67	93.72	69.94	93.28	68.44	**100**
	MD	54.44	65.11	62.33	73.61	63	87.44	72.61	88.44	93.28	74.06	90.56
	SVM	50.48	82.46	60.49	75.66	63.71	93.73	63.1	78.4	91.37	79.49	72.51
	kNN	53.59	77.76	61.03	77.04	66.51	95.18	73.16	77.93	91.48	76.63	91.03
Specificity (%)	**LDA**	60.44	84	61.56	53.5	55.72	**100**	35.61	98.5	89.78	81	62
	QDA	60.22	86.17	71.94	57.78	69.94	97.39	42.39	94.22	89.78	86.11	69.61
	MD	59.28	95.89	76.06	80.56	75.72	94.39	68.28	81.44	97.39	79.67	77.22
	SVM	37.1	80.36	64.21	76.93	69.54	87.01	61.52	84.37	90.8	73.56	69.62
	kNN	52.04	87.91	75.9	65.07	72.21	91.89	70.62	89.04	93.11	80.71	70.6

Table 4. Classification rates, sensitivities, specificities (%) for symmetric Itakura distance (model order 6)

		Session										
		1	**2**	**3**	**4**	**5**	**6**	**7**	**8**	**9**	**10**	**11**
Classification rates (%)	**LDA**	45	85	61.67	71.67	66.67	83.33	51.67	46.67	85	75	80
	QDA	63.33	**90**	63.33	88.33	68.33	81.67	86.67	60	86.67	70	80
	MD	61.67	88.33	68.33	88.33	68.33	81.67	83.33	61.67	85	63.33	76.67
	SVM	48.33	88.33	70	83.33	66.67	85	76.67	61.67	86.67	75	78.33
	kNN	59.44	85.56	55.56	82.78	61.11	82.5	75.83	60	84.17	71.94	76.67
Sensitivity (%)	**LDA**	34.67	89.39	69.44	82.67	74.11	81.56	64.06	54.89	81.28	69.72	93.06
	QDA	78.83	89.39	72.06	97.39	85.33	84.17	**98.5**	44.78	81.28	64.94	93.06
	MD	41.67	77.5	67.11	97.39	70.17	84.83	85.61	74.33	81.28	80.28	88.94
	SVM	61.88	87.44	62.43	84.01	63.51	90.39	77.53	63.63	82.88	69.84	68.3
	kNN	64.2	87.07	56.11	89.57	60.2	84.21	76.84	57.51	81.87	82.88	80.23
Specificity (%)	**LDA**	55.28	91.56	45.5	64.06	63.67	76.5	49.67	32.67	90.78	84.72	65.33
	QDA	47.61	96.33	48.83	76.83	61.72	65.44	86.17	54.22	91.44	88.33	65.33
	MD	67.72	**97**	64.94	76.83	72.44	63.94	92.44	45.33	89.94	41.44	65.33
	SVM	54.94	86.7	63.59	88.5	64.94	80.54	75.83	61.08	89.34	64.64	59.86
	kNN	52.02	88.89	56.21	79.57	67.7	74.6	87.64	57.51	88.46	59.86	72.43

Table 5. Classification rates, sensitivities, specificities (%) for symmetric Itakura distance (model order 10)

		Session										
		1	2	3	4	5	6	7	8	9	10	11
Classification rates (%)	LDA	40	83.33	61.67	76.67	60	90	63.33	80	91.67	86.67	88.33
	QDA	50	85	68.33	81.67	68.33	85	66.67	83.33	91.67	88.33	**91.67**
	MD	51.67	83.33	66.67	83.33	61.67	85	66.67	71.67	90	73.33	83.33
	SVM	40	85	75	81.67	75	88.33	66.67	80	88.33	88.33	90
	kNN	52.78	85.28	71.94	80.56	69.72	90.28	63.33	76.11	86.94	83.33	82.78
Sensitivity (%)	LDA	24.39	92.39	59.11	86.5	72.44	81	79.17	62.06	96.06	69.22	**100**
	QDA	57.11	89.11	63.06	82.17	83.72	81	68.61	62.06	96.06	76.83	**100**
	MD	48.56	68.83	53.94	82.17	75.78	85.94	52.56	67.67	95.39	86.61	82.5
	SVM	47.98	75.38	65.87	80.86	60.83	87.36	60.93	70.21	86.54	76.82	65.6
	kNN	49.42	78.5	70.59	82.64	67.93	90.21	61.97	66.61	86.3	79.46	84.84
Specificity (%)	LDA	64.11	57.61	73.61	71.67	61.56	**100**	41.44	93.56	84.78	92.39	77.28
	QDA	51.5	78.78	69	76.89	55.28	94.11	46.94	98.5	84.78	92.39	84.17
	MD	61	89.78	76.61	77.56	55.28	91.11	70.5	77.39	84.78	64.39	84.17
	SVM	43.53	80.04	66.39	81.98	79.37	89.01	63.59	75.9	89.16	84.72	64.47
	kNN	55.59	81.53	67.52	77.58	68.26	85.53	60.33	84.08	87.72	77.43	82.59

Table 6. Classification rates, sensitivities, specificities (%) for modulation_rhythm Alpha_Alpha and Theta_Alpha

			Session									
			1	2	3	4	5	6	7	8	9	10	11
Alpha_Alpha	Classification rates (%)	LDA	54	51.5	58.5	55	58.5	55.5	72.5	52.5	65.5	59	53
		QDA	66	74.5	65	69	66.5	71.5	86	60	86.5	69.5	51.5
		MD	59	64	70	73.5	69	74	85	51	75	69	54.5
		SVM	66.5	73.5	78.5	76	72.5	79	83	61.5	86	71.5	66.5
		kNN	66.33	79.5	83	83	82.17	81.83	82.92	72.83	**92.75**	82.83	73.33
	Sensitivity (%)	LDA	66.12	78.32	65.92	23.43	83.92	60.8	33.78	32.57	34.83	51.17	54.08
		QDA	49.1	80.8	41.35	32.87	32.62	87.12	36.47	30.12	67.4	67.28	28.1
		MD	46.43	50.08	68.22	65.7	68.45	61.78	47.75	25	74.22	49	64.4
		SVM	60.85	66.72	79.92	79.36	81.28	83.83	81.97	73.71	**93.62**	80.37	59.16
		kNN	63.18	76.52	79.77	74.5	81.34	80.05	79.79	64.37	80.63	77.13	69.72
	Specificity (%)	LDA	16.9	31.62	40.1	76.77	37.85	43.9	78.82	73.88	75.88	69.35	30.25
		QDA	43.37	44.22	80.08	92.52	86.52	68.7	93.15	69.68	82.08	65.77	89.43
		MD	57.87	74.75	64.18	39.57	61	90.18	56.78	77.48	79.03	88.35	56.32
		SVM	68.31	84.22	78.79	79.27	80.96	72.91	82.48	53.69	85.73	72.69	76.77
		kNN	70.74	81.27	82.32	84.41	79.8	74.98	84.07	60.25	**86.71**	79.45	79.01
Theta_Alpha	Classification rates (%)	LDA	49	56.5	54	50.5	56.5	50.5	56.5	55.5	57	59	42.5
		QDA	52	61.5	61.5	62	59.5	76	65.5	52	76	64.5	58
		MD	52	62.5	63.5	51.5	65.5	77	55.5	51	77.5	66.5	59.5
		SVM	54.5	56	69.5	68.5	67.5	73	69.5	56.5	76.5	66	56.5
		kNN	67.83	81	83.25	77	80.58	83.58	79.58	74.25	**86.17**	80.67	73.17
	Sensitivity (%)	LDA	62.2	64.22	69.3	61.67	75.38	46.53	73.92	40.75	59.6	54.57	69.63
		QDA	70.63	84.72	75.43	61.35	88.15	72.42	89.17	37.6	81.05	65.25	78.9
		MD	40.07	47.02	58.3	73.33	65.97	79.73	88.08	68.77	**87.58**	83.68	37.45
		SVM	61.78	72.89	74.66	71.4	74.52	77.9	77.32	68.06	83.82	69.22	69.73
		kNN	63.18	76.52	79.77	74.5	81.34	80.05	79.79	64.37	80.63	77.13	69.72
	Specificity (%)	LDA	53.48	47.55	49.52	56.25	48.1	66.83	86.42	66.42	77.1	66.03	39.98
		QDA	60.18	66.17	51.48	74.83	50.2	69.68	87.57	80.15	**88.55**	79.3	27.45
		MD	73.03	85.42	77.62	72.15	73.05	67.95	87.17	38.63	66.42	55.83	70.35
		SVM	68.4	77.39	78.58	71.51	76.74	85.86	71.05	72.09	87.15	76.19	69.34
		kNN	68.01	82.89	81.1	69.07	75.16	86.35	75.87	75.51	87.69	82.6	71.94

Table 7. Classification rates, sensitivities, specificities (%) for phase locking value (PLV)

		Session										
		1	2	3	4	5	6	7	8	9	10	11
Classification rates (%)	LDA	68.98	63.02	63.02	64.36	62.29	55.84	67.64	61.19	65.33	58.64	67.64
	QDA	69.46	67.4	66.18	69.22	64.6	63.5	68.49	74.21	69.34	60.95	69.83
	MD	68.73	66.67	66.55	65.94	65.09	63.14	68.73	72.75	68.61	60.95	66.91
	SVM	76.76	75.43	70.32	72.14	71.41	69.95	77.98	78.71	75.55	74.57	78.35
	kNN	80.01	77.13	78.04	77.23	77.43	75.49	81.33	**85.06**	80.11	79.95	80.47
Sensitivity (%)	LDA	73.02	62.24	60.58	61.97	60.72	59.36	72.89	62.35	69.21	56.72	64.5
	QDA	78.08	63.85	70.61	70.63	70.8	67.03	70.53	76.16	71.41	61.55	64.04
	MD	72.36	74.8	58.59	46.61	58.38	80.43	83.18	80.7	79.13	64.1	78.71
	SVM	77.72	77.58	70.85	71.04	72.48	77.43	82	**84.82**	77.52	74.81	80.03
	kNN	80.54	76.45	73.44	72.72	74.28	76.42	82.15	84.58	81.88	78.8	80.51
Specificity (%)	LDA	64.2	61.77	64.84	65.92	63.56	56.36	66.5	60.89	63.2	62.24	70.84
	QDA	61.59	68.47	59.65	64.83	57.01	65.75	69.87	73.76	67.21	58.72	77.53
	MD	65.96	58.07	73.61	80.77	73.27	51.63	55.83	65.94	57.92	58.13	56.02
	SVM	76.65	72.03	78.11	76.54	77.86	68.68	76.47	80.03	76.27	76.69	75.94
	kNN	77.87	74.06	79.57	77.92	77.92	71.16	75.92	**83.06**	74.27	77.83	74.88

Table 8. Classification rates, sensitivities, specificities (%) for phase lag index (PLI)

		Session										
		1	2	3	4	5	6	7	8	9	10	11
Classification rates (%)	LDA	60.83	65.09	61.19	58.27	62.29	55.23	66.67	61.92	66.55	58.64	67.27
	QDA	71.78	68	61.8	62.53	64.23	63.14	73.84	71.29	66.55	60.95	70.19
	MD	70.07	67.64	62.41	60.22	60.95	59.73	69.59	71.05	65.57	62.29	70.19
	SVM	77.25	73.24	71.78	69.59	73.11	67.4	80.05	76.64	71.65	73.11	77.98
	kNN	82.14	76.68	77.23	72.55	75.63	74.49	83.31	**85.16**	76.72	74.96	80.41
Sensitivity (%)	LDA	60.17	64.05	64.08	60.33	63.5	57.65	70.96	66.37	67.88	60.64	63.8
	QDA	76.95	66.59	71.91	74.86	70.45	59.65	75.54	73.94	66.86	65	62.51
	MD	63.18	78.65	51.25	34	45.63	71.64	82.1	83.14	72.55	66.37	81.64
	SVM	77.57	78.5	69.05	63.64	71.1	74.23	83.02	81.66	77.09	73.28	81.16
	kNN	81.25	78.03	71.29	66.41	70.16	77.58	84.06	**87.16**	76.35	74.37	81.89
Specificity (%)	LDA	58.68	64.1	59.18	57.11	62.05	51.08	61.65	59.3	62.85	60.4	70.26
	QDA	68.24	71.41	54.77	51.96	55.07	65.37	71.03	69.15	67.61	56.36	75.69
	MD	75.11	58.61	74.21	**86.69**	74.45	47.16	54.13	61.85	57.83	59.16	56.71
	SVM	80.71	73.13	78.87	75.36	76.96	70.02	77.42	80.44	73.14	71.98	77.41
	kNN	80.59	74.22	77.5	73.68	79.07	66.77	77.24	78.85	72.6	74.31	75.91

Table 9. Classification rates, sensitivities, specificities (%) for weighted phase lag index (wPLI)

		Session										
		1	2	3	4	5	6	7	8	9	10	11
Classification rates (%)	LDA	56.08	54.38	54.87	54.14	53.41	53.16	58.15	55.84	50.36	55.6	56.08
	QDA	56.81	64.11	60.1	60.34	62.65	60.22	60.34	57.79	56.45	60.83	56.08
	MD	56.2	51.7	55.6	57.42	56.08	56.81	60.1	57.06	58.15	57.91	56.81
	SVM	66.55	67.88	72.14	66.91	**72.87**	67.76	66.3	66.67	66.3	62.29	67.27
	kNN	67.19	63.56	69.57	67.7	69.02	69.28	71.74	67.17	68.65	66.95	68.69
Sensitivity (%)	LDA	51.4	56.37	49.24	53.75	50.75	51.02	52.49	51.09	50.02	49.07	57.94
	QDA	53.76	81.28	54.01	49.58	53.32	69.18	50.15	58.56	52.5	45.27	71.14
	MD	34.65	10.17	87.43	78.02	**90.55**	40.12	66.41	59.42	66.55	63.8	44.35
	SVM	59.79	52.76	75.71	71.15	75.47	63.45	71.26	68.12	66.94	66.23	64.61
	kNN	61.16	53.41	78.32	71.33	77.94	60.05	71.52	67.96	67.14	67.21	62.76
Specificity (%)	LDA	60.76	54.78	57.03	54.76	53.85	56.41	61.99	63.35	50.68	57.3	57.6
	QDA	62.21	47.89	72.02	69.83	71.57	53.38	70.94	59.68	59.99	75.49	42.96
	MD	78.07	**95.84**	25.12	32.85	21.79	75.77	56.17	57.09	49.5	51.42	72.41
	SVM	71.03	72.72	59.84	62.31	59.33	71.31	65.48	64.86	66.7	61.34	69.6
	kNN	71.84	72.01	57.78	60.74	57.78	71.96	68.56	63.63	67.5	66.12	70.8

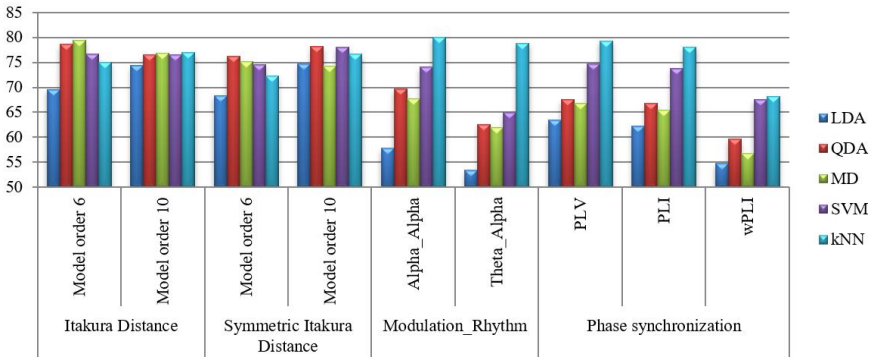

Figure 1. The mean of the classification rates (%)

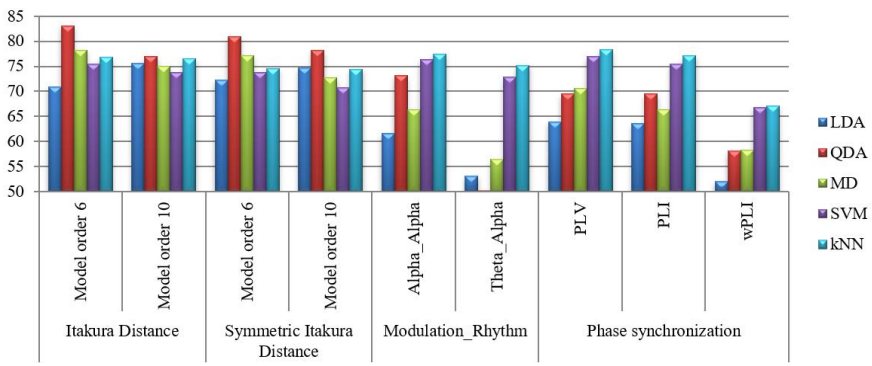

Figure 2. The mean of the sensitivities (%)

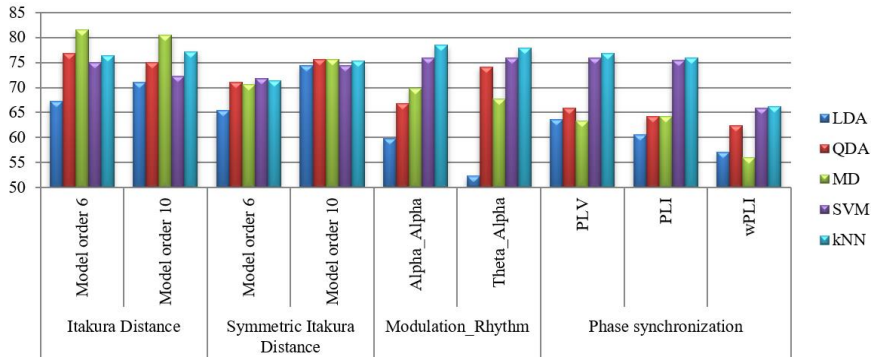

Figure 3. The mean of the specificities (%)

The highest means of sensitivity and specificity were provided by the autoregressive process (Itakura distance as feature vectors for both) with quadratic discriminant analysis and Mahalanobis distance classifier, respectively.

5. CONCLUSIONS

The research evaluated efficiency of the some of the feature extraction methods and classification algorithms for EEG signals recorded from a subject in several sessions in eight years (2012 - 2019), in a motor imagery task paradigm. So, there were not found any systematic enhancement in outcomes when the EEG signals were recorded in the sessions performed in the last years. We may conclude that the subject's training in performing the imagination of the hand movement didn't augment the performance and, maybe, good or bad results were attained due to the subject's physiological determinants.

The highest classification rate of 93.33%, from all the sessions, was attained with Mahalanobis distance based classifier and Itakura distance (no matter the order). The maximum sensitivity was obtained with linear discriminant analysis and quadratic discriminant analysis for Itakura distance, and symmetric Itakura distance model order 10. The specificity of 100% was achieved with Itakura distance, model order 10 and linear discriminant analysis.

Regarding the mean of the classification rates, the best result was achieved using k nearest neighbor classifier and amplitude modulation energy index (in the case of alpha modulation band of alpha rhythm) as feature vector. A near result was found for Mahalanobis distance classifier and autoregressive process by means of Itakura distance of order 6. As the sensitivities and specificities had high values for both cases, any of them would be a valuable choice in an on-line brain-computer interface paradigm.

The future work involves, on one hand, recording of many sessions of EEG signals from the same subject in order to determine if the biological factors (like fatigue, feeling thirst or hungry) affects the performance, on the other hand, manipulating a feature vector as a weighted combination of the measures used in this paper and involving further EEG channels like CP3 and CP4 along with the already used ones.

REFERENCES

[1] Shih, J.J., Krusienski, D.J., Wolpaw, J.R. (2012). Brain-computer interfaces in medicine. In Mayo Clinic Proceedings, Elsevier, 87(3): 268-279. https://doi.org/10.1016/j.mayocp.2011.12.008

[2] Mudgal, S.K., Sharma, S.S.K., Chaturvedi, I., Sharma, A. (2020). Brain Computer Interface advancement in Neurosciences: Applications and Issues. Interdisciplinary Neurosurgery, 100694. https://doi.org/10.1016/j.inat.2020.10069

[3] Ramadan, R.A., Vasilakos, A.V. (2017). Brain computer interface: control signals review. Neurocomputing, 223: 26-44. https://doi.org/10.1016/j.neucom.2016.10.024

[4] Aggarwal, S., Chugh, N. (2019). Signal processing techniques for motor imagery brain computer interface: A review. Array, 1: 100003. https://doi.org/10.1016/j.array.2019.100003

[5] Pfurtscheller, G., Brunner, C., Schlögl, A., Da Silva, F.L. (2006). Mu rhythm (de) synchronization and EEG single-trial classification of different motor imagery tasks. NeuroImage, 31(1): 153-159. https://doi.org/10.1016/j.neuroimage.2005.12.003

[6] Tariq, M., Trivailo, P.M., Simic, M. (2018). Motor imagery based EEG features visualization for BCI applications. Procedia Computer Science, 126: 1936-1944. https://doi.org/10.1016/j.procs.2018.08.057

[7] McFarland, D.J., Krusienski, D.J., Wolpaw, J.R. (2006). Brain–computer interface signal processing at the Wadsworth Center: mu and sensorimotor beta rhythms. Progress in Brain Research, 159: 411-419. https://doi.org/10.1016/S0079-6123(06)59026-0

[8] McCane, L.M., Heckman, S.M., McFarland, D.J., Townsend, G., Mak, J.N., Sellers, E.W., Vaughan, T.M. (2015). P300-based brain-computer interface (BCI) event-related potentials (ERPs): People with amyotrophic lateral sclerosis (ALS) vs. age-matched controls. Clinical Neurophysiology, 126(11): 2124-2131. https://doi.org/10.1016/j.clinph.2015.01.013

[9] Hoffmann, U., Vesin, J.M., Ebrahimi, T., Diserens, K. (2008). An efficient P300-based brain–computer interface for disabled subjects. Journal of Neuroscience Methods, 167(1): 115-125. https://doi.org/10.1016/j.jneumeth.2007.03.005

[10] Erkan, E., Akbaba, M. (2018). A study on performance increasing in SSVEP based BCI application. Engineering Science and Technology, an International Journal, 21(3): 421-427. https://doi.org/10.1016/j.jestch.2018.04.002

[11] Saravanakumar, D., Reddy, M.R. (2019). A high performance hybrid SSVEP based BCI speller system. Advanced Engineering Informatics, 42: 100994. https://doi.org/10.1016/j.aei.2019.100994

[12] Volosyak, I., Gembler, F., Stawicki, P. (2017). Age-related differences in SSVEP-based BCI performance. Neurocomputing, 250: 57-64. https://doi.org/10.1016/j.neucom.2016.08.121

[13] Song, X., Yoon, S.C. (2015). Improving brain–computer interface classification using adaptive common spatial patterns. Computers in Biology and Medicine, 61: 150-160. https://doi.org/10.1016/j.compbiomed.2015.03.023
[14] Ansari, M.F., Edla, D.R., Dodia, S., Kuppili, V. (2019). Brain-Computer Interface for wheelchair control operations: An approach based on Fast Fourier Transform and On-Line Sequential Extreme Learning Machine. Clinical Epidemiology and Global Health, 7(3): 274-278. https://doi.org/10.1016/j.cegh.2018.10.007
[15] Zhou, B., Wu, X., Ruan, J., Zhao, L.V., Zhang, L. (2019). How many channels are suitable for independent component analysis in motor imagery brain-computer interface. Biomedical Signal Processing and Control, 50: 103-120. https://doi.org/10.1016/j.bspc.2019.01.017
[16] Li, X., Fan, H., Wang, H., Wang, L. (2019). Common spatial patterns combined with phase synchronization information for classification of EEG signals. Biomedical Signal Processing and Control, 52: 248-256. https://doi.org/10.1016/j.bspc.2019.04.034
[17] Wu, T., Yan, G.Z., Yang, B.H., Sun, H. (2008). EEG feature extraction based on wavelet packet decomposition for brain computer interface. Measurement, 41(6): 618-625. https://doi.org/10.1016/j.measurement.2007.07.007
[18] McFarland, D.J., Wolpaw, J.R. (2008). Sensorimotor rhythm-based brain–computer interface (BCI): Model order selection for autoregressive spectral analysis. Journal of Neural Engineering, 5(2): 155-62. https://doi.org/10.1088/1741-2560/5/2/006
[19] www.gtec.at, accessed on 7 Jan. 2020.
[20] Dornhege, G., Millán, J.D.R., Hinterberger, T., McFarland, D.J., Muller, K.R. (2007). Toward brain-computer interfacing (Vol. 63). Cambridge, MA: MIT press.
[21] Kong, X., Thakor, N., Goel, V. (1995). Characterization of EEG signal changes via Itakura distance. Proceedings of 17th International Conference of the Engineering in Medicine and Biology Society, 2: 873-874. https://doi.org/10.1109/IEMBS.1995.579247
[22] Estrada, E., Nazeran, H., Ebrahimi, F., Mikaeili, M. (2009). Symmetric Itakura distance as an EEG signal feature for sleep depth determination. In Summer Bioengineering Conference, American Society of Mechanical Engineers, 48913: 723-724. https://doi.org/10.1115/SBC2009-206233
[23] Gysels, E., Celka, P. (2004). Phase synchronization for the recognition of mental tasks in a brain-computer interface. IEEE Transactions on Neural Systems and Rehabilitation Engineering, 12(4): 406-415. https://doi.org/10.1109/TNSRE.2004.838443
[24] Gonuguntla, V., Wang, Y., Veluvolu, K.C. (2013). Phase synchrony in subject-specific reactive band of EEG for classification of motor imagery tasks. In 2013 35th Annual International Conference of the IEEE Engineering in Medicine and Biology Society (EMBC), Osaka, Japan, pp. 2784-2787. https://doi.org/10.1109/EMBC.2013.6610118
[25] Stam, C.J., Nolte, G., Daffertshofer, A. (2007). Phase lag index: assessment of functional connectivity from multi channel EEG and MEG with diminished bias from common sources. Human Brain Mapping, 28(11): 1178-1193. https://doi.org/10.1002/hbm.20346
[26] Vinck, M., Oostenveld, R., Van Wingerden, M., Battaglia, F., Pennartz, C.M. (2011). An improved index of phase-synchronization for electrophysiological data in the presence of volume-conduction, noise and sample-size bias. Neuroimage, 55(4): 1548-1565. https://doi.org/10.1016/j.neuroimage.2011.01.055
[27] Eva, O.D., Lazar, A.M. (2019). Amplitude modulation index as feature in a brain computer interface. Traitement du Signal, 36(3): 201-207. https://doi.org/10.18280/ts.360301
[28] Zhang, R., Xu, P., Guo, L., Zhang, Y., Li, P., Yao, D. (2013). Z-score linear discriminant analysis for EEG based brain-computer interfaces. PloS One, 8(9): e74433. https://doi.org/10.1371/journal.pone.0074433
[29] Lotte, F., Congedo, M., Lécuyer, A., Lamarche, F., Arnaldi, B. (2007). A review of classification algorithms for EEG-based brain–computer interfaces. Journal of Neural Engineering, 4(2): R1.
[30] Cincotti, F., Mattia, D., Babiloni, C., Carducci, F., Bianchi, L., del RJ, M., Babiloni, F. (2002). Classification of EEG mental patterns by using two scalp electrodes and Mahalanobis distance-based classifiers. Methods of Information in Medicine, 41(4): 337-341.
[31] Kevric, J., Subasi, A. (2017). Comparison of signal decomposition methods in classification of EEG signals for motor-imagery BCI system. Biomedical Signal Processing and Control, 31: 398-406. https://doi.org/10.1016/j.bspc.2016.09.007
[32] Luo, J., Gao, X., Zhu, X., Wang, B., Lu, N., Wang, J. (2020). Motor imagery EEG classification based on ensemble support vector learning. Computer Methods and Programs in Biomedicine, 105464. https://doi.org/10.1016/j.cmpb.2020.105464
[33] Bansal, D., Mahajan, R. (2019). EEG-Based Brain-Computer Interfaces: Cognitive Analysis and Control Applications. Academic Press. https://doi.org/10.1016/b978-0-12-814687-3.00002-8
[34] Gubert, P.H., Costa, M.H., Silva, C.D., Trofino-Neto, A., (2020). The performance impact of data augmentation in CSP-based motor-imagery systems for BCI applications. Biomedical Signal Processing and Control, 62: 102152. https://doi.org/10.1016/j.bspc.2020.102152